ACS APPLIED MATERIALS & INTERFACES

Research Article

www.acsami.org

Impact of Oxygen Plasma Treatment on the Device Performance of Zinc Oxide Nanoparticle-Based Thin-Film Transistors

Hendrik Faber,[†] Johannes Hirschmann,[†] Martin Klaumünzer,[‡] Björn Braunschweig,[‡] Wolfgang Peukert,[‡] and Marcus Halik*,[†]

[†]Organic Materials & Devices (OMD), Department of Materials Science, University Erlangen-Nürnberg, Martensstraße 7, 91058 Erlangen, Germany

[‡]Institute of Particle Technology, Dept. of Chemical and Biological Engineering, University Erlangen-Nürnberg, Cauerstraße 4, 91058 Erlangen, Germany

Supporting Information

ABSTRACT: Thin-films of zinc oxide nanoparticles were investigated by photoluminescence spectroscopy and a broad defect-related yellow-green emission was observed. Oxygen plasma treatment was applied in order to reduce the number of defects, and the emission intensity was quenched to 4% of the initial value. Thin-film transistors that incorporate the nanoparticles as active semiconducting layers show an improved device performance after oxygen plasma treatment. The maximum drain current and the charge carrier mobility increased more than 1 order of magnitude up to a nominal value of 23 $cm^2 V^{-1} s^{-1}$ and the threshold voltage was lowered.

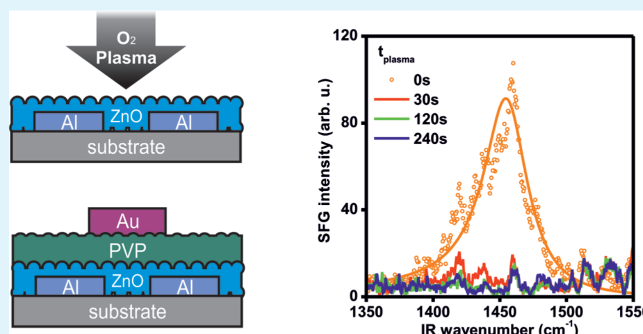

KEYWORDS: *zinc oxide, nanoparticles, plasma treatment, thin-film transistors*

INTRODUCTION

Solution processing of metal oxides as active components in electronic applications has been the subject of heightened importance in recent years[1] and is considered as a key technology to realize the production of electronic devices on flexible substrates for low-cost and large-area market segments. Among the range of different processing techniques, the use of dispersible nanoparticles is a promising approach. Nanoparticles benefit from a range of size-related properties (e.g., high surface area, band gap tuning), which can be tailored to specific needs. However, to improve certain characteristics, e.g., to enhance conductivity, the application of postdeposition treatments is often necessary for particle-based systems. Those treatments can involve high temperatures, which are incompatible with applications on flexible substrates.[2,3]

The wide band gap II–VI compound semiconductor zinc oxide is a promising inexpensive and nontoxic material, which can be prepared in a variety of different nanoscale geometries (including particles,[4] rods,[5] or wires[6]) and afterward processed via dispersions. Because of the synthesis conditions, however, the resulting nanoscaled ZnO is not free of diverse defects.[7] Owing to the large surface-to-volume ratio surface defects play a predominant role in controlling device performances. These can be detected in photoluminescence (PL) studies, where a broad emission in the visible spectrum (~530 nm) is observed besides the band gap related excitonic peak in the ultraviolet (UV) region. Although this kind of defect related green-to-yellow emission is well-known and documented for various ZnO systems in literature, the exact determination of its origin is still under debate. Among the possible causes, oxygen vacancies are named most prominently,[8,9] but also zinc interstitials,[10] impurity atoms,[11] or surface states.[12] Nevertheless, such defects are prone to limit the performance of electronic devices and consequently methods for their elimination are of interest.

In this work, we report on a postdeposition oxygen plasma treatment on nanoparticulate zinc oxide layers and its impact on the device performance of thin-film transistors in top-gate configuration.

EXPERIMENTAL DETAILS

Zinc oxide nanoparticles with a diameter of approximately 5 nm covered by an acetate ligand shell (<1 nm) were synthesized in a hydrolysis reaction as described previously.[13,14] The formation of homogeneous and smooth (root-mean-square roughness <1.4 nm) ZnO particulate layers was achieved by spin-casting from an ethanolic dispersion with subsequent drying at 100 °C for 6 min. A film thickness of only one monolayer, i.e., 5–6 nm, was determined in previous experiments.[13]

To monitor the changes on the ZnO particle layer, optical studies on the emission properties related to the defect density were conducted using a FluoroLog 3 spectrofluorometer (Horiba Jobin Yvon GmbH), which is equipped with a double-grating on the

Received: December 22, 2011
Accepted: February 22, 2012
Published: March 5, 2012

 © 2012 American Chemical Society

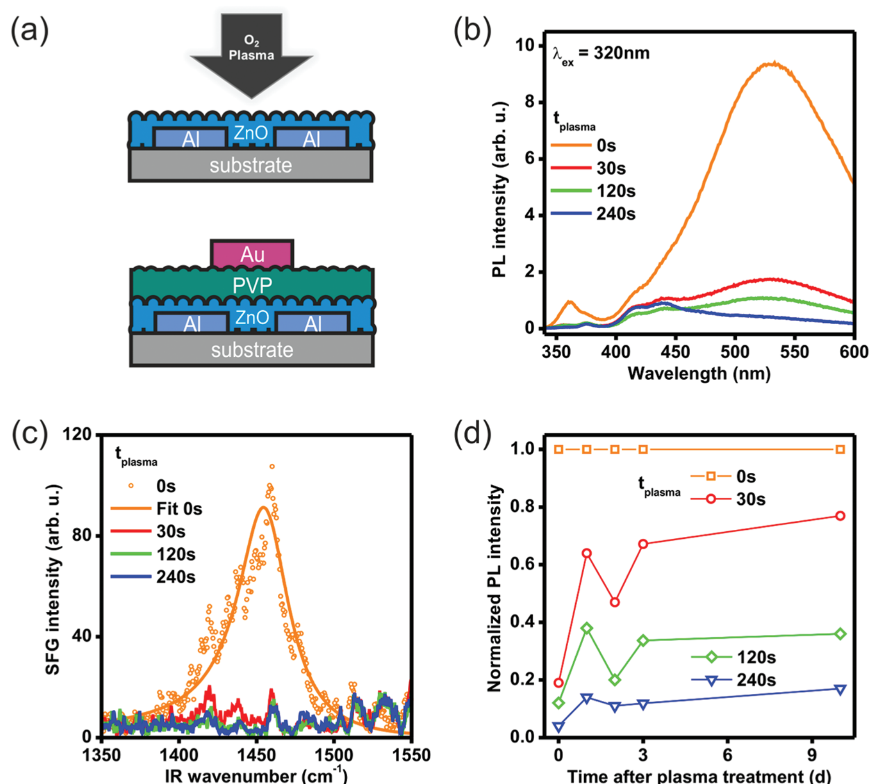

Figure 1. (a) Top: Schematic representation of the plasma treatment during the fabrication process. Bottom: Transistor setup. (b) Photoluminescence emission spectra of untreated (t_{plasma} = 0 s) and plasma treated ZnO NP layers. The excitation wavelength λ_{ex} was 320 nm. (c) SFG signals corresponding to the carboxylate group for untreated and plasma treated particle layers. (d) The recovery of the defect intensity over time. The maxima of the defect peaks related to different exposure times were normalized to the intensity of the untreated sample for each respective measurement time after the plasma treatment.

excitation as well as on the emission side. Measurements were taken directly on films within the process flow of thin-film transistor (TFT) device fabrication (prior to the deposition of the dielectric, Figure 1a).

Oxygen plasma treatments of different intensities, varied by time of exposure (30, 120, or 240 s), were applied to the ZnO NP layer with the intention to reduce the defect emission (in particular oxygen vacancies). During the process the oxygen pressure in the plasma chamber (Diener electronic "Pico", 200 W) was set to 0.2 mbar. The temperature in the chamber did not exceed 120 °C.

To reveal changes in the ligand shell after O_2 plasma treatment of thin ZnO particle layers, vibrational sum-frequency generation (SFG) was additionally applied. SFG has been shown to be a useful nondestructive method to study and characterize the molecular composition of surfaces, interfaces and thin layers.[15,16] Surface energy determination was carried out using three different fluids (water, diiodomethane, formamide) according to the Owens−Wendt−Kaelble method.

The impact of the postdeposition plasma treatment on the TFT performance was investigated by implementing plasma treated and nontreated ZnO layers in top-gated TFTs. Aluminum source-drain and gold gate electrodes were deposited and patterned by thermal evaporation through a stencil mask. The ratio of channel width W to channel length L equals 15 for all devices. The semiconductor and the 190 nm dielectric polymer layer (poly(4-vinylphenol), PVP) were both deposited by spin coating.[17,18] During TFT fabrication, the O_2 plasma was applied to the ZnO NP layer prior to the deposition of the dielectric layer. Electrical measurements were performed with an Agilent B1500A parameter analyzer in ambient air.

■ RESULTS AND DISCUSSION

Photoluminescence studies of pristine NP layers (t_{plasma} = 0 s) show the broad defect-related emission in the visible spectrum with a maximum intensity at λ_{max} = 528 nm (see Figure 1b), which decreases depending on the plasma exposure time t_{plasma}. For exposure times of 30, 120, and 240 s, a decrease to about 19, 12, and 4% of the initial intensity was observed. The shape and λ_{max} of the spectra did not change significantly with exposure, indicating the same origin of the emission. The declining intensity suggests the reduction of defect density.

Impurity atoms inside the ZnO nanoparticles as well as zinc interstitials were among the possible defects responsible for the visible emission, as proposed in literature. However, the ballistic impact of oxygen species during the plasma exposure must be seen as statistical rather than systematic or targeted. A preferential removal of impurities or elimination of zinc interstitials was thus considered improbable and both kinds of defects were dismissed as the cause for green emission within our ZnO particle system.

The application of oxygen plasma to various ZnO systems (nanowires, particles, bulk films) has been reported to reduce the charge carrier concentration and conductivity.[19−22] This was explained by a reduction of oxygen vacancies[19,23] as well as adsorption of oxygen on the ZnO surface. In the adsorption process, oxygen species retrieve an electron from the ZnO and in turn induce a depletion layer.[22,23] The role of oxygen vacancies as the source of green PL emission in ZnO is controversial. Despite reports that negate their involvement,[24] Ra et al. demonstrated that ZnO nanowires featured a strong visible PL emission for a high concentration of oxygen vacancies, whereas the emission was greatly suppressed for low vacancy concentrations.[25] Therefore, oxygen vacancies are

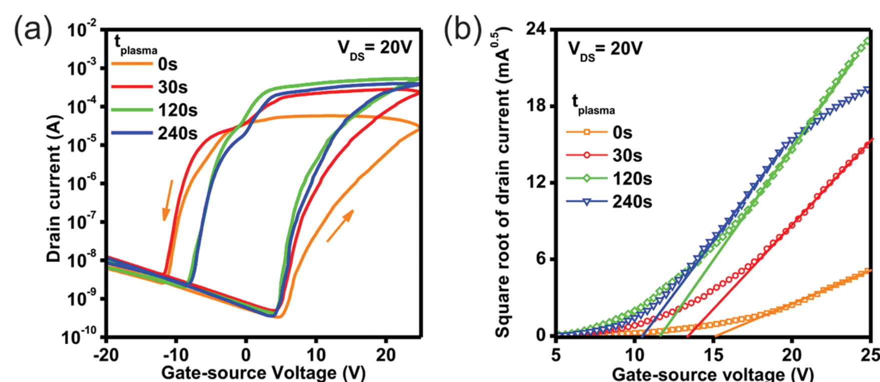

Figure 2. (a) Transfer characteristics of nanoparticle based top-gate TFTs with untreated and plasma treated ZnO layers. (b) Plot of square root of I_D over V_{GS} with the determination of V_{TH}.

considered to be at least a possible cause for the visible PL emission within this work.

Because of the synthesis conditions, the NPs are covered by an acetate ligand shell that can be responsible for defect states on the particle surface. Therefore, removing the ligand shell alters the surface states and can decrease the PL defect emission. This effect of reduced visible PL intensity was observed by Sakohara et al. after firing an acetate covered ZnO particle membrane at 350 °C.[26] In a recent study, Sharma at al. additionally linked the green emission of ZnO NPs to the presence of acetate as well as hydroxyl groups on the particle surface after their synthesis.[27] These groups are therefore considered to be the most probable candidates for causing the defect emission in our NP system.

For the untreated sample, the SFG spectrum in Figure 1c is dominated by a vibrational band centered at an infrared (IR) wavenumber of 1450 cm^{-1} due to carboxylate (COO^-) symmetric stretching vibrations of acetate adsorbed on the ZnO particle surfaces.[28,29] Already for oxygen plasma exposure times as short as 30 s, the SFG intensity of the acetate band decreases substantially to negligible values which is indicative for a complete removal of the ligand shell.

To investigate the origin of the PL quenching we have monitored all samples over time (storing in ambient air) and rerecorded the PL spectra (Figure 1d). For all plasma-treated samples we obtained a recovery of the PL defect emission. The recovery is increases with decreasing plasma exposure time, although not reaching the intensity of the untreated sample. During the storage in ambient conditions, atmospheric water can be the source for the attachment of hydroxyl groups on the ZnO surface, which in turn are believed to cause the increased visible emission.[27]

Surface energy determinations of particle layers featured an increase from an initial value of 63 to 67 mN m^{-1} after O_2 plasma exposure which decreased to 57 mN m^{-1} after one week of storage in air.

These findings suggest that the reduced PL emission after O_2 plasma exposure is predominantly caused by the removal of acetate and possibly hydroxyl groups, while the recovery is attributed to the formation hydroxyl groups from atmospheric water.

The plasma treatment is applied to the ZnO nanoparticulate layer just prior to the deposition of the PVP dielectric. Hence, changes inflicted by the plasma treatment directly address the semiconductor/dielectric interface, which is essential for device performance. From the time scale of recovery (Figure 1d) we estimate that the effect of plasma treatment is still significant during the short exposure to ambient air between plasma treatment and PVP deposition.

The transfer characteristics for plasma treated and nontreated devices (Figure 2a) feature a full gate-source voltage (V_{GS}) sweep (forward direction from −20 to +25 V and backward from +25 to −20 V). For the untreated devices (pristine ZnO layers without plasma exposure), a typical n-type transistor behavior was observed with a drain current (I_D) modulation by application of a positive gate bias in forward-sweep direction. The backward sweep, however, reveals a bistable hysteresis of more than 20 V, originating from interface effects at the contact area between ZnO and PVP.[18] Because of the hysteresis and the apparent deviation from common transistor behavior, characteristic values such as the field-effect mobility may not be suitable for comparison with common TFTs without bistable hysteresis, but are still useful for internal comparison within the given system. The effective charge carrier mobility μ of 2 $cm^2\ V^{-1}\ s^{-1}$ and drain current on/off ratio of 8×10^4, extracted from the forward sweep, are in agreement with previous results.[13,18]

Introducing the O_2 plasma treatment in the TFT fabrication process leads to significant improvements in the device performance (see summary of characteristic values in Table I). While the turn-on voltage and the off current in the I_D-V_{GS} plot stay rather constant at approximately 4.5 V and 4×10^{-10}A, the maximum drain currents increase significantly. In turn, the mobility is enhanced over an order of magnitude, reaching a maximum value of 23.8 $cm^2\ V^{-1}\ s^{-1}$ for t_{plasma} = 120 s. This improvement was facilitated by the overall reduction of defect states and especially the ligand shell removal, which allowed improved interparticular current transport. We note, that the increased device performance is not attributed to changes in morphology. Investigations by atomic force microscopy did not show significant changes after plasma

Table I. Summary of Characteristic Values Extracted from Untreated and Plasma-Treated ZnO Nanoparticle-Based TFTs

t_{plasma} (s)	μ ($cm^2\ V^{-1} s^{-1}$)	V_{TH} (V)	on/off	S (V dec^{-1})	N_{trap} ($cm^{-2} V^{-1}$)
0	2.2	15.4	8×10^4	1.44	2.4×10^{12}
30	13.4	13.3	4×10^5	1.29	2.2×10^{12}
120	23.8	11.6	1×10^6	0.67	1.1×10^{12}
240	19.9	10.3	1×10^6	1.11	1.9×10^{12}

dx.doi.org/10.1021/am2018223 | ACS Appl. Mater. Interfaces 2012, 4, 1693−1696

exposure and still featured low roughness values (rms less than 1.4 nm).

The common method to determine the threshold voltage V_{TH} by plotting the square root of I_D over V_{GS} and extrapolation of the linear part to the *x*-axis is depicted in Figure 2b. With increasing plasma exposure time, V_{TH} is continuously shifting to smaller values from initial 15.4 to 10.2 V. This trend is in contrast to reports in literature, where a positive shift for ZnO based TFTs was found after O_2 plasma treatment.[19,22] However, the charge transport in devices of this special setup does not only rely on channel formation but also on charging the NP-dielectric interface. This effect occurs as parallel process and makes it difficult to compare the turn-on behavior to common TFT devices.[18]

Since transistors are interface controlled devices, the maximum trap density per interfacial area was estimated according to refs 30 and 31 using

$$N_{trap} = \left[\frac{qS\log(e)}{kT} - 1\right]\frac{C_A}{q}$$

with Boltzmann constant k, temperature T, and the elementary charge q. The area normalized capacitance C_A is given by $\varepsilon_0\varepsilon_r/d$, with the electric constant ε_0, relative permittivity ε_r (3.6 for PVP), and dielectric layer thickness d. The subthreshold swing S decreases from an initial 1.4 to a minimum of 0.7 V dec^{-1} at t_{plasma} = 120 s. As the maximum trap density correlates with the development of S, it is also reduced after the plasma treatment from an initial value of 2.4×10^{12} cm^{-2} V^{-1} to a minimum of 1.1×10^{12} cm^{-2} V^{-1} for t_{plasma} = 120 s.

In contrast to the PL emission, which decreases monotonically with increasing plasma exposure, the subthreshold swing and the estimated maximum trap density slightly increase again for the longest t_{plasma} = 240 s. The positive impact on the device performance due to the elimination of the ligand shell and compensation of oxygen vacancies reaches a maximum at t_{plasma} = 120 s. For longer exposure times, the plasma treatment is assumed to create oxygen containing adsorbates (O^-, O^{2-},OH^-) at the ZnO surface, which then act as trapping sites.[21]

CONCLUSION

In conclusion, the O_2 plasma treatment of ZnO NP layers leads to a significantly reduced defect emission and the removal of the particles' acetate ligand shell. This results in an enhanced switching behavior (improved subthreshold swing) in the corresponding top-gated TFT devices. Additionally, the extracted field-effect mobility increased significantly by 1 order of magnitude to a maximum value of 23.8 cm^2 V^{-1} s^{-1}. Therefore, the relatively simple plasma treatment is an effective way to improve the device performance of particle based systems without the need of high temperatures.

ASSOCIATED CONTENT

Supporting Information

AFM images (PDF). This material is available free of charge via the Internet at http://pubs.acs.org.

AUTHOR INFORMATION

Corresponding Author

*E-mail: marcus.halik@ww.uni-erlangen.de.

Notes

The authors declare no competing financial interest.

ACKNOWLEDGMENTS

Financial support was provided by the Research Training Group 1161—"Disperse Systems for Electronic applications", which is funded by Deutsche Forschungsgemeinschaft (DFG) and Evonik Degussa GmbH, Germany. B.B. is grateful for support by the Alexander von Humboldt foundation and a Feodor Lynen fellowship.

REFERENCES

(1) Jeong, S.; Moon, J. *J. Mater. Chem.* **2012**, *22*, 1243−1250.
(2) Lee, S.; Jeong, S.; Kim, D.; Park, B. K.; Moon, J. *Superlattices Microstruct.* **2007**, *42*, 361.
(3) Gross, M.; Linse, N.; Maksimenko, I.; Wellmann, P. J. *Adv. Eng. Mater.* **2009**, *11* (4), 295−301.
(4) Meulenkamp, E. A. *J. Phys. Chem. B* **1998**, *102*, 5566−5572.
(5) Voigt, M.; Klaumünzer, M.; Thiem, H.; Peukert, W. *J. Phys. Chem. C* **2010**, *114*, 6243−6249.
(6) Vayssieres, L. *Adv. Mater.* **2003**, *15*, 464.
(7) Schmidt-Mende, L.; MacManus-Driscoll, J. L. *Mater. Today* **2007**, *10*, 40−48.
(8) Vanheusden, K.; Seager, C. H.; Warren, W. L.; Tallant, D. R.; Voigt, J. A. *Appl. Phys. Let.* **1996**, *68*, 403−405.
(9) Djurišić, A. B.; Leung, Y. H. *Small* **2006**, *2*, 944−961.
(10) Korsunska, N. O.; Borkovska, L. V.; Bulakh, B. M.; Khomenkova, L. Y.; Kushnirenko, V. I.; Markevich, I. V. *J. Lumin.* **2003**, *102−103*, 733−736.
(11) Garces, N. Y.; Wang, L.; Bai, L.; Giles, N. C.; Halliburton, L. E.; Cantwell, G. *Appl. Phys. Lett.* **2002**, *81*, 622−624.
(12) Djurišić, A. B.; Choy, W. C. H.; Roy, V. A. L.; Leung, Y. H.; Kwong, C. Y.; Cheah, K. W.; Rao, T. K. G.; Chan, W. K.; Lui, H. F.; Surya, C. *Adv. Funct. Mater.* **2004**, *14*, 856−864.
(13) Faber, H.; Klaumünzer, M.; Voigt, M.; Galli, D.; Vieweg, B. F.; Peukert, W.; Spiecker, E.; Halik, M. *Nanoscale* **2011**, *3*, 897−899.
(14) Marczak, R.; Segets, D.; Voigt, M.; Peukert, W. *Adv. Powder Technol.* **2010**, *21*, 41−49.
(15) Shen, Y. R. *Nature* **1989**, *337*, 519−525.
(16) Lagutchev, A.; Lozano, A.; Mukherjee, P.; Hambir, S. A.; Dlott, D. D. *Spectrochim. Acta, Part A* **2010**, *75*, 1289−1296.
(17) Halik, M.; Klauk, H.; Zschieschang, U.; Schmid, G.; Radlik, W.; Weber, W. *Adv. Mater.* **2002**, *14*, 1717−1722.
(18) Faber, H.; Burkhardt, M.; Jedaa, A.; Kälblein, D.; Klauk, H.; Halik, M. *Adv. Mater.* **2009**, *21*, 3099−3104.
(19) Lee, S.; Bang, S.; Park, J.; Park, S.; Jeong, W.; Jeon, H. *Phy. Status Solidi A* **2010**, *207*, 1845−1849.
(20) Ra, H. W.; Khan, R.; Kim, J. T.; Kang, B. R.; Bai, K. H.; Im, Y. H. *Mater. Lett.* **2009**, *63*, 2516−2519.
(21) Ra, H.-W.; Im, Y.-H. *Nanotechnology* **2008**, *19*, 485710.
(22) Walther, S.; Polster, S.; Jank, M. P. M; Thiem, H.; Ryssel, H.; Frey, L. *Adv. Powder Technol.* **2011**, *22*, 253−256.
(23) Liu, M.; Kim, H. K. *Appl. Phys. Lett.* **2004**, *84*, 173−175.
(24) McCluskey, M. D.; Jokela, S. J. *J. Appl. Phys.* **2009**, *106*, 071101.
(25) Ra, H. W.; Choi, K. S.; Ok, C. W.; Jo, S. Y.; Bai, K. H.; Im, Y. H. *Appl. Phys. Lett.* **2008**, *93*, 033112.
(26) Sakohara, S.; Tickanen, L. D.; Anderson, M. A. *J. Phys. Chem.* **1992**, *96*, 11086−11091.
(27) Sharma, A.; Singh, B. P.; Dhar, S.; Gondorf, A.; Spasova, M. *Surf. Sci.* **2012**, *606*, L13−L17.
(28) Braunschweig, B.; Mukherjee, P.; Kutz, R. B.; Wieckowski, A.; Dlott, D. D. *J. Chem. Phys.* **2010**, *133*, 234702.
(29) Schrödle, S.; Moore, F. G.; Richmond, G. L. *J. Phys. Chem. C* **2007**, *111*, 8050−8059.
(30) Zhang, L.; Li, J.; Zhang, X. W.; Jiang, X. Y.; Zhang, Z. L. *Thin Solid Films* **2010**, *518*, 6130−6133.
(31) McDowell, M.; Hill, I. G.; McDermott, J. E.; Bernasek, S. L.; Schwartz, J. *Appl. Phys. Lett.* **2006**, *88*, 073505.